Coagulation of bentonite suspension by polyelectrolytes or ferric chloride: floc breakage and reformation

Elise Barbot, Philippe Dussouillez, J.Y. Bottero, Philippe Moulin

Coagulation of bentonite suspension by polyelectrolytes or ferric chloride: Floc breakage and reformation

E. Barbot[a], P. Dussouillez[b], J.Y. Bottero[b], P. Moulin[a,*]

[a] M2P2 UMR 6181, CNRS, Aix-Marseille Université, Laboratoire de Mécanique, Modélisation et Procédés Propres, Europôle de l'Arbois, BP 80, Bâtiment Laennec, Hall C, 13545 Aix en Provence Cedex 04, France
[b] CEREGE UMR 6635, CNRS, IRD, Aix-Marseille Université, Collège de France, Europôle de l'Arbois, BP 80, 13545 Aix en Provence Cedex 04, France

Coagulation process usually involves different hydrodynamic conditions, in particular when it is followed by a filtration step. In this study, coagulation performance was investigated under a wide range of shear stress. Floc behaviour was followed in-line by laser granulometry to determine size distribution and structure. Synthetic suspension of bentonite in tap water was used as a reference for mineral solids in surface water. Three cationic polymers (polyamine based and polyDADMAC) and ferric chloride were tested using different coagulation reactor geometries. Jar-test indicated coagulation performance under mild hydrodynamic conditions and Taylor–Couette reactors were used to create shear stresses up to 8 Pa. Flocs formed with ferric chloride are not able to grow under middle shear stress like 1.5 Pa. On the contrary, polyelectrolytes lead to large flocs, dense (D_f = 2.6) and resistant to shear stress. A qualitative comparison of floc resistance to shear depending on hydrodynamic conditions and coagulant type is given through the calculation of the strength factor. Fractal dimension measurements indicate a mechanism of particle erosion when flocs are subjected to a higher shear stress in Taylor–Couette reactor. Floc re-growth is also investigated, and breakage appears to be non-reversible regardless of coagulant and conditions experimented.

1. Introduction

Coagulation processes remain ubiquitous in water treatment. Within these systems floc characteristics dictate treatment performance. Amongst these size, structure, and settling velocity have primary importance. It is well established nowadays that floc formation and breakage depends on several parameters such as coagulant type and concentration, coagulation time and hydrodynamics in the reactor given its geometry and mixing type. During the effluent treatment process (mixing and filtration), flocs are subjected to a wide range of shear stresses that lead to a change of their characteristic with time.

Thus, during the past decade, studies have focused on coagulation in stirred tanks and the evolution of floc characteristics during the process [1–9]. Spicer et al. presented different works on floc change depending on the impeller type and the rotating speed of the impeller [2,3]. During the coagulation of polystyrene particles by alum in a baffled standard tank equipped with a rushton turbine, they found a decrease of steady-state floc size with increasing shear rate. An increase of fractal dimension with an increase of the velocity gradient G is generally found [4,10]. Li et al. found that fractal dimension varies with G following a power law, independent on the coagulation mechanism [10].

However, shear stresses cannot be accurately controlled in these reactors. Spicer et al. highlighted that the floc size depends on the gradient velocity but also on the circulation time, varying depending on the impeller type (radial or axial) [2]. Bouyer et al. determined experimentally the local hydrodynamic conditions in a jar and focused on the relation between those and floc size [8]. Taylor–Couette reactors offer a solution to this problem by utilizing two concentric cylinders where the rotation of the inner cylinder involves a shear of the fluid contained in the annular space [11–13]. In this geometry rotation speed controls shear rate and it can be maintained homogeneously throughout experiments.

Even though mineral coagulants remain the most used in industrial processes, polyelectrolyte flocculants were developed because of several advantages [14]. For example, the use of such compounds leads to a high turbidity, COD and BOD_5 removal [15]. Additionally, efficiency does not depend on effluent pH and sludge volume is reduced in comparison to processes utilizing mineral coagulants. However, because of the high cost of polyelectrolytes, combinations of metal salts and polymers are often used to converge the advantages of both types of coagulant [15–17]. Another advantage of organic coagulants versus mineral ones results from the

* Corresponding author. Tel.: +33 4 42 90 85 01; fax: +33 4 42 90 85 15.
E-mail address: philippe.moulin@univ-cezanne.fr (P. Moulin).

Nomenclature

D	impeller diameter (m)
D_f	fractal dimension
D_{modal}	modal diameter (μm)
$F(q)$	form factor
G	shear rate (s^{-1})
$I(q)$	scattered intensity
n_0	refractive index
n_s	refractive index of the scatterer
$\bar{n}$	mean optical index
P_0	power number of the impeller
q	wave vector (nm^{-1})
R_1	external radius of the inner cylinder (m)
R_2	internal radius of the external cylinder (m)
Re	Reynold number
$S(q)$	structure factor
Ta	Taylor number
ε	turbulent energy dissipation rate ($m^2\,s^{-3}$)
λ_0	wavelength (nm)
ν	kinematic fluid viscosity ($m^2\,s^{-1}$)
θ	scattering angle (rad)
τ_p	shear stress (Pa)
Ω	rotating speed (rad s^{-1})

difference in aggregation mechanism, which imparts different floc structure. With metal salts, the main coagulation mechanisms are, depending on pH, formation of amorphous hydroxide precipitate or charge neutralization characterized by the formation of short bridges [18]. Charge neutralization is also involved when polyelectrolytes are used, but the polymeric chains create a bridging between particles through generally longer bridges [19,20]. This specific mechanism confers to the floc a better resistance to shear. Li et al. calculated floc strength for flocs formed under three coagulation mechanisms. They found that bridging coagulation give the strongest flocs, while floc strength formed under charge neutralization is the weakest [10]. Jarvis et al. experimented the effect of the addition of polyDADMAC to ferric chloride for the coagulation of reservoir water. The polymer leads to the formation of more resistant flocs to shear stress [9]. Floc reformation after breakage is also highly correlated to coagulant type and therefore coagulation mechanism [7,9].

In the present work, the suspension studied is bentonite in water. Amongst the wide range of applications of clay minerals, bentonite is used to create synthetic suspensions in membrane fouling studies. This clay is chosen to achieve 100% particle rejection with fouling solely due to cake deposit [21–23]. Moreover, bentonite represents natural surface water turbidity appropriately, and its colloidal and rheological properties are well defined [24]. Results of cross-flow ultrafiltration of a suspension of bentonite in tap water are presented in a former study [25]. This former work focuses on performance of a coagulation–ultrafiltration hybrid process in terms of membrane fouling.

The aim of the current paper is to determine more specifically coagulation performance of bentonite suspension in terms of floc behaviour. Several hydrodynamic conditions are investigated to reproduce the different shear stresses that flocs can encounter during a membrane filtration process. Coagulation is performed in different reactors to create a wide range of shear stresses. Mineral and organic coagulants are tested, with floc structure and size being determined in-line by light scattering. Floc behaviour is followed during breakage and reformation.

2. Materials and methods

2.1. Apparatus

The raw water was a mixture of tap water and bentonite (CECA, Clarsol) at 0.2 and 1 g L^{-1} (turbidity = 80 NTU and 300 NTU, respectively). Bentonite pellets aggregates due to the ionic strength of the tap water. This suspension is thus characterized by floculi around 30 μm in size. The tap water is characterized by a pH of 7.5–7.9, and a conductivity of 0.035 mS cm^{-1}. The calcium concentration is about 62 mg L^{-1}, the magnesium concentration is at 4.8 mg L^{-1} and sodium is at 20.4 mg L^{-1}. Such a suspension was chosen to simulate conditions found in natural surface water where clay particles are already aggregated. Four coagulants were tested. The suspension at 1 g L^{-1} was also used for the determination of coagulant performance toward turbidity removal. Ferric chloride (13% Fe) was selected as the most used and well-known coagulant in drinking water production. Three cationic polymers C577, C591 and C595 (Cytec) were also tested. The first is polyamine based (dimethylamine epichlorohydrin ethylenediamine polymer) with a medium molecular weight. The two other polymers contain polyDADMAC (polydiallyldimethyl ammonium chloride) and C591 and C595 have molecular weight high and very high, respectively. They were diluted 1:100 in distilled water before utilization, and the diluted solution was kept only 1 week, in order to avoid any degradation. pH control was achieved by addition of hydrochloric acid.

Three different coagulation reactors were utilized in this study: a Jar and two Taylor–Couette reactors. Jar-tests were performed in a flocculator (type 10008, Fisherbrand), with four blades 2.5 cm large and 7.5 cm length. The mixing velocity ranged from 20 to 200 rpm. One-litre beakers were used, each one measured 13 cm high with an internal diameter of 10 cm. The coagulation was performed in three steps: a rapid mixing at 200 rpm for 2 min, floc growth at 40 rpm for 10 min and floc breakage at 200 rpm for 3 min. The average velocity gradient G, or shear rate, is calculated as follows (1):

$$G = \left(\frac{\varepsilon}{\nu}\right)^{1/2} \quad (1)$$

where ν is the kinematic viscosity of the suspending fluid, and ε is the average turbulent energy dissipation rate (2):

$$\varepsilon = \frac{P_0 \Omega^3 D^5}{V} \quad (2)$$

where P_0 is the impeller power number, Ω the rotating speed, D the impeller diameter and V the tank volume. At 40 rpm, the flow is laminar whereas it is turbulent at 200 rpm.

The two Taylor–Couette reactors are composed of two concentric cylinders where the inner cylinder (radius R_1) rotates and the outer one (radius R_2) is stationary. Their characteristics are given in Fig. 1. Their external dimensions are the same, but they present different gap width and rotating speed Ω, which enable different shear stresses to be examined.

In the reactor A, coagulation was performed under a turbulent flow at the maximum rotating speed, creating a shear stress of 1.5 Pa. In the reactor B, shear stress reaches 7.8 Pa for a maximal rotating speed of 330 rpm. Table 1 details shear stress and shear rate for each reactor and each rotating speed. Gap width in reactor B (e_B = 0.2 cm) is considerably smaller than in reactor A (e_A = 1.5 cm) to limit the turbulence involved by the high rotating speed. Information is given about the hydrodynamic condition through the calculation of the Reynolds (3) and Taylor number (4):

$$\mathrm{Re} = \frac{\Omega R_1 (R_2 - R_1)}{\nu} \quad (3)$$

$$\mathrm{Ta} = \frac{R_1 \Omega^2 (R_2 - R_1)^3}{\nu^2} \quad (4)$$

Table 1
Hydrodynamic conditions in each coagulation reactor (*shear rates in this reactor have not been determined).

Geometry	Rotating speed (rpm)	Shear rate (s^{-1})	Shear stress (Pa)	Reynolds number	Taylor number
Jar-test	40	30	0.3		
	200	260	–		
Taylor–Couette reactor A	100	250	1.5	15,700	37,011
Taylor–Couette reactor B	60	*	0.6	1,400	35,700
	100	*	1.3	2,400	99,100
	150	*	2.4	3,500	223,100
	200	*	3.6	4,700	396,500
	330	*	7.8	7,800	1079,600
	400	*	10	9,500	1586,200

For the lowest rotating speeds, the flow is laminar. When the Taylor number reaches a critical value (Ta_c), the flow becomes unstable. A good approximation of Ta_c is given by Taylor [26]. For the conditions experimented in this work, the flow is turbulent. More information about the Taylor–Couette reactor A can be found in the work of Coufort et al. [13].

2.2. Analyses

Floc size and structure are determined using a laser granulometer Mastersizer S (Malvern Instruments). It measures particle size from 50 nm to 900 μm and results are presented in volume percentage. The suspension is introduced in the granulometer cell by a peristaltic pump placed after the cell. Floc geometry is now commonly described as fractal, implying that aggregates are self-similar and scale invariant. The fractal dimension (D_f) defined in three dimension ranges 1–3, and gives information on aggregate structure. Fractal dimensions close from 1 characterize open and highly branched structures, whereas fractal dimensions close from 3 reveal very compact and spherical aggregates. Fractal dimension is often determined by light scattering, which enable rapid and in-line measurement. This method involves measurement of light intensity I as a function of the wave vector q, where q is defined as follows (5):

$$q = |\vec{q}| = \frac{4\pi n_0}{\lambda_0}\ \sin\left(\frac{\theta}{2}\right) \tag{5}$$

where n, θ and λ are the refractive index of the medium, the scattered angle and wavelength of radiation in vacuum, respectively. It has been shown that for a mass fractal aggregate, which satisfies the conditions for Rayleigh–Gans–Debye (RGD) regime, its scattered intensity I is described by the following equation (6):

$$I(q) \propto q^{-D_f} \tag{6}$$

Fractal dimension of flocs is calculated using the method developed by Lambert et al. for initial particles whose size is close to the scattering wavelength [27]. Multiple scattering is taken into account by introducing the mean optical index $\bar{n}$. This index characterizes the mean optical environment of particles belonging to the fractal object. A scatterer mean optical contrast is therefore defined as the optical contrast between scatterers and their mean environment: $n_s/\bar{n}$. The angular scattered intensity is given by (7):

$$I(q) \propto F(q).S(q) \tag{7}$$

$F(q)$ is the form factor and can be calculated as the Mie angular scattered intensity by a primary particle in a fractal geometry characterized by the scatterer mean optical index $n_s/\bar{n}$. $S(q)$ is the structure factor and depends only on the spatial arrangement of the particles in the aggregate. $S(q)$ is therefore proportional to q^{-D_f}. The fractal dimension is then calculated using this structure factor, as the slope of the log $S(q)$ versus log (q) curve (Fig. 2).

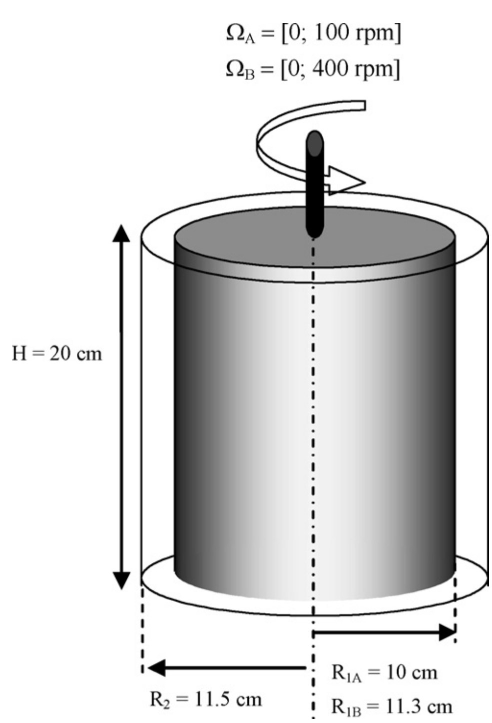

Fig. 1. Dimensions of Taylor–Couette reactors A and B.

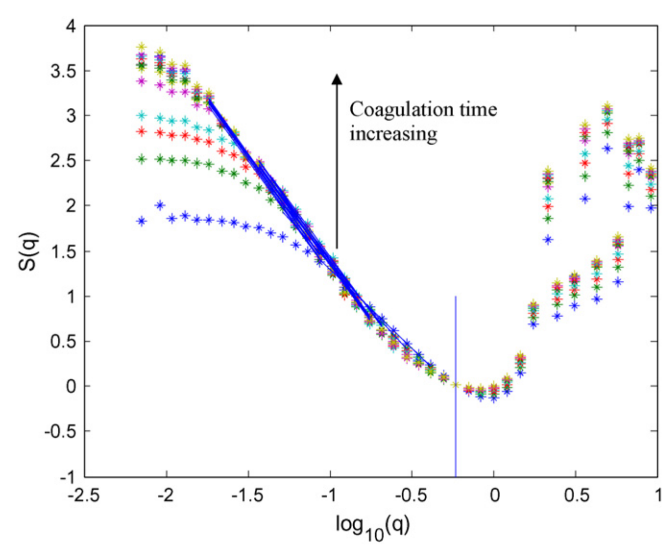

Fig. 2. Variation of structure factor versus wave vector on a log-log scale [Jar-test, C595, 0.39 ppm].

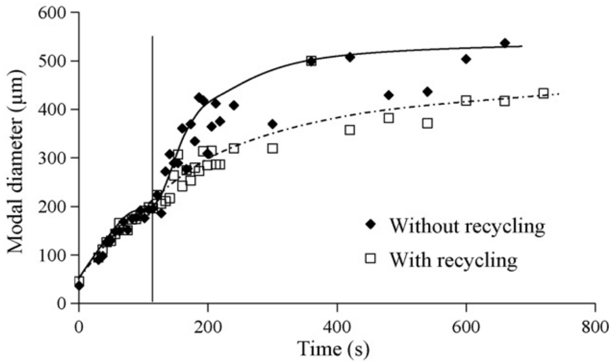

Fig. 3. Variation of floc size versus time depending on the protocol [Jar-test, C595, 0.39 ppm].

2.3. Coagulation protocols

Different coagulation parameters (coagulant injection mode and effect of shear in the peristaltic pump) were carefully studied to achieve a good reproducibility, depending on the type of reactor used. In Jar-test, coagulant is classically injected into the suspension under high rotating speed to perform a rapid mixing. However, this protocol is not necessarily the best when Taylor–Couette reactor is used. The specific geometry of this type of reactor coupled with the use of a polymeric coagulant may involve reproducibility issues. Two injection modes were investigated. Coagulant can be introduced in the reactor after the suspension as it is performed during Jar-test, or on the contrary a solution of coagulant is poured into the reactor and a small volume of concentrated suspension is then introduced. The first method involved a difference in floc size about 50 µm, whereas the second method gave highly reproducible results. However, the dimensions of reactor B, in particular the small gap width, did not allow this protocol to be followed. Experiments with this reactor B were multiplied two times to insure reproducibility.

After the measurement in the granulometer, suspension can be either reinjected in the reactor or thrown away. This second method obviously limits the number of measurements but the first method involves a possible floc breakage by the peristaltic pump. Effect of suspension recycling was investigated for the three reactors. In Jar-test, there was no difference between the two protocols during the first step of the experiment (rapid mixing at 200 rpm). When rotating speed was decreased, an important floc breakage occurred if the suspension was recycled, and floc size was decreased of 100 µm compared to the protocol without recycling (Fig. 3). In Taylor–Couette reactor B, effect of recirculation was tested at different rotating speed. Volumic floc size distributions after 30 min of coagulation under 150 and 200 rpm are presented in Fig. 4. The effect of shear by the pump can be neglected compared to shear that occurs in the reactor. Consequently, the protocol chosen for experiments in Taylor–Couette reactor implies a recirculation of the suspension after measurement. Thus, a specific protocol was selected for each reactor, considering the imposition due to their geometry.

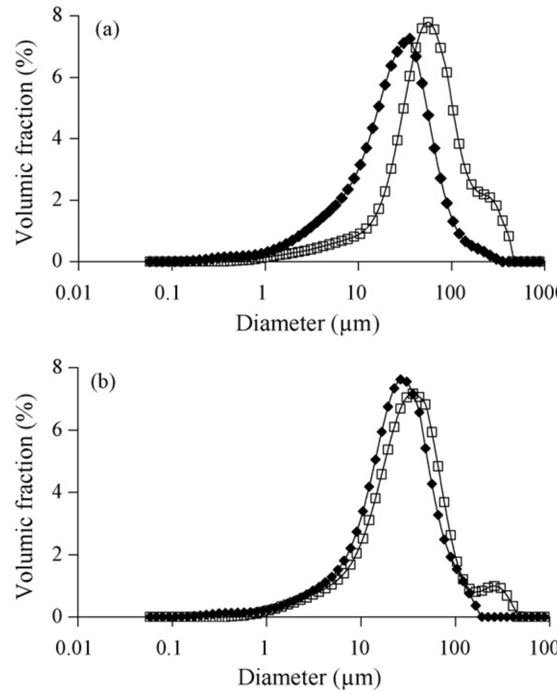

Fig. 4. Floc size distribution depending on the protocol: (♦) without recycling of suspension and (□) with recycling. (a) 150 rpm and (b) 200 rpm [reactor B, coagulant C595 at 0.15 ppm, t = 30 min].

3. Results and discussion

3.1. Coagulant performance

Jar-tests were performed to determine coagulant optimal concentration in terms of turbidity removal. After the slow mixing step, suspension was poured into a 1 L graduated cylinder to follow floc settling. Considering the low bentonite concentration, no interface between sludge and supernatant was visible, making the establishment of Kynch's curves impossible. To compare settling velocities at different concentrations of coagulant, 10 mL samples of supernatant were collected during the decantation and turbidity was monitored versus time. Table 2 gathers supernatant turbidity after 30 min of decantation for each coagulant. For two polyelectrolytes, two concentrations were selected due to their high performance in terms of both turbidity removal and settling velocity. For the two bentonite concentration tested, each coagulant gives excellent results in terms of turbidity removal, which ranges 70–99%.

Table 2
Optimal coagulant concentration and supernatant turbidity after 30 min of decantation.

Coagulant	Bentonite at 0.2 g L^{-1}		Bentonite at 1 g L^{-1}	
	Concentration (ppm)	Turbidity (NTU)	Concentration (ppm)	Turbidity (NTU)
C577	0.196	2	0.98	8
	0.49	4	1.47	4
C591	0.19	4	0.76	8
C595	0.15	2	0.39	4
	0.39	4	0.78	3
$FeCl_3$	2.6	8	5.2	11

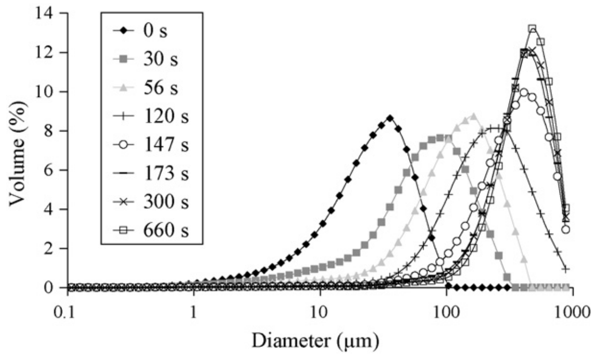

Fig. 5. Variation of floc size distribution with time [Jar-test, C595 at 0.15 ppm].

3.2. Coagulation in Jar-test

Floc size distribution was only performed on 0.2 g L^{-1} bentonite suspension. In fact, higher concentrations raised the obscuration above acceptable levels for measurement. Fig. 5 represents floc size distribution during coagulation in Jar-test. The curve at $t = 0$ s corresponds to the bentonite aggregates formed in tap water before addition of coagulant. Due to the effect of ionic strength, bentonite particles aggregate to form floculi. When coagulation starts, floc size distribution remained monomodal. The modal diameter (D_{modal}) was consequently chosen to define floc size variations in this paper. Flocs reach their maximum size after 6 min and then the polydispersity of the suspension decreases. For each coagulant, two phases of growth are noticed (Fig. 6). During the two first minutes of rapid mixing when polyelectrolytes are tested, floc size increases and starts to stabilize. Then when the rotating speed of the impeller is reduced, flocs are able to grow even further until their size reaches a maximum value. With ferric chloride, a difference in floc size is noticed during the first step of the Jar-test. First of all, the floc growth is more rapid then when polymers are used, certainly due to the coagulation mechanism involved. After a rapid increase, floc size decreases until the mixing speed is reduced, and then flocs grow slowly. This behaviour is also mentioned in the literature when another mineral coagulant, alum, is used to coagulate latex beads [3]. Organic coagulants rapidly lead to the formation of large flocs, ranging 400–500 µm depending on the type of coagulant and its concentration. Ferric chloride forms smaller flocs (350 µm) that grow more slowly.

A good parameter to quantify floc strength is the floc strength factor, defined as the ratio of floc size after and before breakage at a particular shear rate [28]. Strength factors can only be compared for similar breakage conditions, but it is a simple evaluation

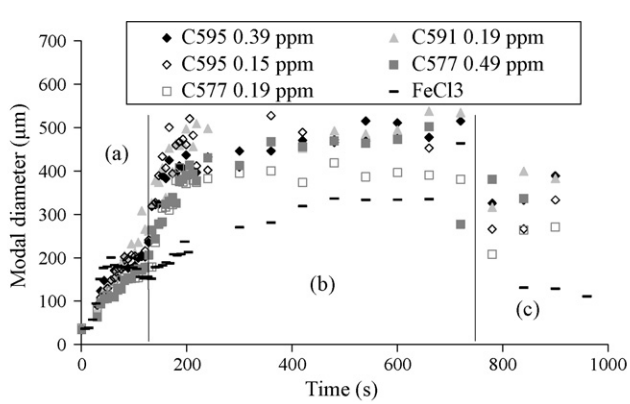

Fig. 6. Variation of modal diameter with time in Jar-test: (a) $\Omega = 200$ rpm, (b) $\Omega = 40$ rpm and (c) $\Omega = 200$ rpm.

Table 3
Floc strength factor for the different coagulants in Jar-test, calculated after 1 min of breakage at 200 rpm.

Coagulant and concentration (mg L^{-1})	Floc strength (%)
C591, 0.19 ppm	63.1
C577, 0.19 ppm	51.0
C577, 0.49 ppm	58.6
C595, 0.15 ppm	61.0
C595, 0.39 ppm	58.0
$FeCl_3$	34.0

of the resistance of flocs to shear. In the review written by Jarvis et al., the authors mentioned the lack of information found in literature about this parameter [29]. Though, it appears as a good parameter to quantitatively compare the performance of the different coagulants and flocculants in each reactor presented in this study. Table 3 gives the strength factor obtained in Jar-test for an increase of shear rate from 30 to 260 s^{-1}. Polyelectrolytes lead to the formation of flocs presenting a strength factor from 51 to 63%. Flocs formed with polyelectrolytes C591 and C595 are the more resistant. Flocs formed with C577 seem to be more fragile. However, flocs formed by ferric chloride are the less resistant, since they are characterized by a 34% strength factor.

Differences between organic coagulants and ferric chloride are also noticed in terms of structure. Fractal dimensions of flocs formed by polyelectrolytes are higher than for flocs formed with ferric chloride (Table 4). This result is in agreement with floc resistance. When the rotating speed is finally increased (200 rpm) after the 10 min of slow mixing, flocs formed with organic coagulants are less broken than flocs formed with ferric chloride. Thus polyelectrolytes enable the formation of larger, more compact and more resistant flocs than ferric chloride.

Information on coagulation mechanism can be obtained from the $\log(I)$–$\log(q)$ curves. When ferric chloride is used, curves in the q range of [−4; −1.8] does not change (Fig. 7a). It means that floc structure remains constant during coagulation. When polymers are used, these curves show a significant evolution (Fig. 7b). The initial concave curve obtained by light scattering of a bentonite suspension slowly becomes convex after polyelectrolyte addition, showing that floc structure is highly modified during the coagulation process. Final structure is clearly different from the initial structure of bentonite floculi formed by action of the ionic strength of tap water. Ferric chloride only gathers floculi without modifying them, whereas polyelectrolytes seem to destabilize floculi and form flocs of complete different structure.

3.3. Coagulation in Taylor–Couette reactor

Coagulation in Taylor–Couette reactor A was performed at a constant rotating speed of 100 rpm and a shear stress of 1.5 Pa. A rapid floc growth occurs regardless of coagulant, and a difference in floc size between ferric chloride and polyelectrolytes is only noticeable after 2 min (Fig. 8). Polyelectrolytes lead to large flocs, whose size reach a plateau at 300 s. When ferric chloride is used, flocs grow until they reach a size for which breakage is no more negligible. After a rapid growth until 200 µm, floc size decreases slowly, as it occurred during the Jar-test. Flocs formed by ferric chloride are not allowed to grow under a high shear stress. In contrast, a shear stress of 1.5 Pa is not a limiting factor to growth for flocs induced by polyelectrolytes. Results obtained in this reactor are in agreement with preliminary observations during Jar-test. In particular, ferric chloride creates more porous flocs, easily breakable at a medium shear stress of 1.5 Pa. Structure of flocs formed in the Taylor–Couette reactor is clearly different from structure of flocs obtained during the Jar-test. For coagulant C591, fractal dimension can reach the maximum value of 3 (Table 4). Generally, flocs formed under a shear

Table 4
Fractal dimension depending on coagulation reactor and shear stress [Jar-test, after 10 min at 40 rpm; Taylor–Couette reactor B, after 5 min at 60 rpm; Taylor–Couette reactor A, after 25 min at 100 rpm].

Coagulant	$D_f \pm \sigma$		
	Jar-test τ_p = 0.03 Pa	Reactor B τ_p = 0.6 Pa	Reactor A τ_p = 1.5 Pa
C591, 0.19 ppm	2.5 ± 0.13	2.71 ± 0.03	3.03 ± 0.02
C577, 0.19 ppm	2.63 ± 0.01	2.70 ± 0.10	2.72 ± 0.01
C577, 0.49 ppm	2.60 ± 0.07	2.82 ± 0.04	2.67 ± 0.01
C595, 0.15 ppm	2.65 ± 0.05	2.75 ± 0.01	2.71 ± 0.01
C595, 0.39 ppm	2.64 ± 0.06	2.81 ± 0.05	2.71 ± 0.01
$FeCl_3$	2.23 ± 0.03	–	1.76 ± 0.02

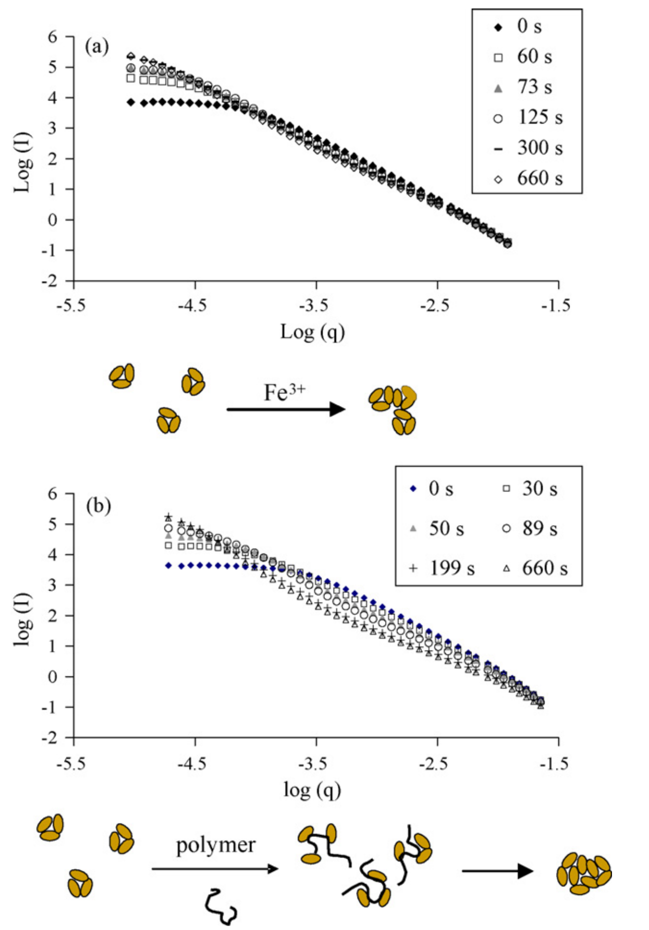

Fig. 7. Variation of log(I) versus log(q) during coagulation in Jar-test: (a) $FeCl_3$ and (b) C595 at 0.15 ppm.

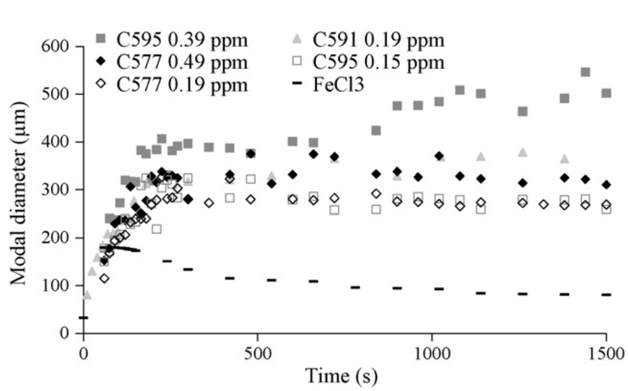

Fig. 8. Variation of flocs modal diameter versus time [Taylor–Couette reactor A, Ω = 100 rpm, τ = 1.5 Pa].

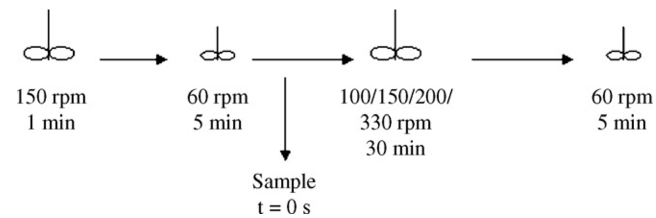

Fig. 9. Shear schedule in Taylor–Couette reactor B.

stress of 1.5 are more compact than those formed under mild conditions in the jar, except for ferric chloride. The shear may induce a rearrangement of particles in the floc, which can lead to denser aggregates through restructuration [30].

Taylor–Couette reactor B was used to first create large flocs under soft hydrodynamic conditions and then follow their behaviour under different shear stresses by increasing the rotating speed. Fig. 9 represents schematically the different steps of the experiment. Floc formation protocol was identical to Jar-test, in the sense that rotating speed of the inner cylinder was set up at a high rate for mixing and then decrease to enable floc growth. Thus bentonite suspension and coagulant were mixed at 150 rpm during a short period. Then the rotating speed was decreased at 60 rpm (τ = 0.6 Pa) during 5 min to allow floc formation and avoid decantation in the reactor. A first measurement by light scattering was performed at t = 0 s just before the increase of rotating speed. A first comparison can be made between the floc characteristics obtained in this reactor B with results obtained during Jar-test and in reactor A (Fig. 10). Even though the reactors have different geometries, evolution of floc size is consistent with shear stress increase. Flocs formed under 0.6 Pa are smaller than those formed under 0.03 Pa and larger than these formed under 1.5 Pa. Fractal dimensions of

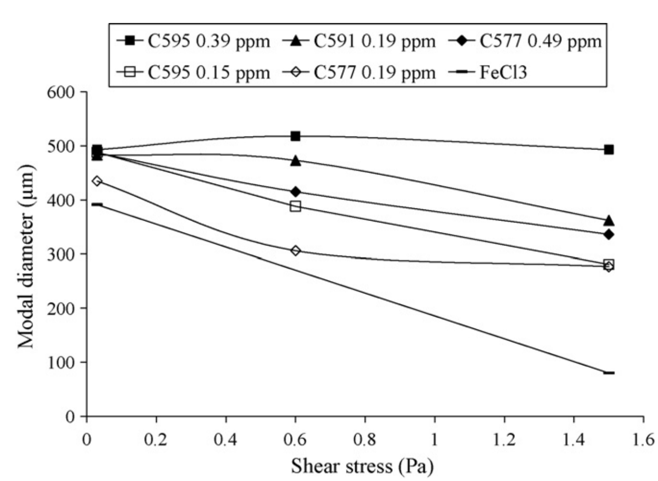

Fig. 10. Variation of flocs modal diameter versus shear stress [Jar-test, after 10 min at 40 rpm; Taylor–Couette reactor B, after 5 min at 60 rpm; Taylor–Couette reactor A, after 25 min at 100 rpm].

Table 5
Floc strength factor after 1 and 30 min and of breakage and floc re-growth after 30 min of breakage depending on shear stress in Taylor–Couette reactor B.

Coagulant	Shear stress (Pa)	Strength factor (%) after 1 min of breakage	Strength factor (%) after 30 min of breakage	Reformation after 30 min (%)
C591, 0.19 ppm	1.3	88.0	38.1	47
	2.4	64.8	17.8	28
	3.6	54.0	9.3	23
	7.8	26.0	9.3	13
C577, 0.19 ppm	1.3	64.3	25.1	35
	2.4	41.3	12.4	29
	3.6	28.0	7.8	24
	7.8	10.0	6.1	15
C577, 0.49 ppm	1.3	–	31.2	52
	2.4	–	18.5	–
	3.6	–	10.1	30
	7.8	–	2.5	18
C595, 0.15 ppm	1.3	68.1	26.5	32
	2.4	53.6	16.1	25
	3.6	37.5	8.3	20
	7.8	13.1	8.0	14
C595, 0.39 ppm	1.3	96.6	44.2	53
	2.4	77.1	21.2	34
	3.6	65.0	13.0	29
	7.8	23.5	3.2	18

flocs formed during the Jar-test and in Taylor–Couette reactor B belong to the same range (Table 4). This validates the flocs formation protocol, and enables the study of their behaviour under higher shear stress.

3.3.1. Floc breakage

After floc growth during 5 min at 60 rpm, rotating speed was increased at 100, 150, 200 or 330 rpm, corresponding to a shear stress of 1.3, 2.4, 3.6 or 7.8 Pa, respectively. For each shear stress, floc size decreases with time (Fig. 11). Floc breakage increases with shear stress, and time to reach steady state decreases when shear stress increases. Thus, initial kinetic floc breakage depends on shear stress but also on the coagulant (Fig. 11a and b) used and its concentration (Fig. 11 b–e). A variation of concentration implies great difference in floc behaviour, even though no difference in size was noticeable during the Jar-test. However, behaviour differences disappear when time and/or shear stress increase.

Coagulant C577 (polyamine) forms flocs which are rapidly broken even at low shear stress. Floc breakage kinetic variation with shear stress shows only a slight increase. On the contrary, coagulants C591 and C595 (polyDADMAC) form more resistant flocs at the lowest shear stress.

Calculations of strength factors at two times during floc break up in the Taylor–Couette reactor B are gathered in Table 5. It is calculated based on the ratio between the floc size after 1 or 30 min of breakage and the size at $t = 0$ s before the breakage. During a filtration step, flocs can be subjected to a high shear stress but only for a short time, for instance when the suspension passes through a pump. The strength factor calculated after 1 min provides information of the floc size after such a step in the treatment line. When shear stress increases, the strength factor decreases invariably. The difference between the two concentrations studied for C595 is obvious and 0.39 ppm appears as the optimal concentration, which did not appear clearly during the Jar-tests. At this optimal concentration, the coagulant C595 creates more resistant flocs than C591. This is likely due to the difference of molecular weight. Even if these polyDADMAC coagulants are highly charged and formed flocs mainly by charge neutralization or electrostatic patch mechanism [20], results indicates that a phenomenon of bridging occurs. C595 has the highest molecular weight, and therefore leads to more resistant flocs.

It is interesting to compare floc size with the Kolmogorov scale η. Coufort et al. [13] highlighted the strong correlation between floc size and Kolmogorov scale for a bentonite suspension coagulated with alum in a Taylor–Couette reactor. For the same geometry than our reactor A, they found the floc size to be between η and 2η. The same result was obtained in our case when ferric chloride was used. The floc size after stabilization reaches 80 μm for a corresponding Kolmogorov scale about to 55 μm. However, when polyelectrolytes are used, floc size remains larger than the Kolmogorov scale, since the floc size ranges from 300 to 500 μm.

3.3.2. Mechanism of floc breakage

The mechanism of floc breakage can be analyzed from Fig. 12 and particularly looking at the curves around q value of 10. When aggregation increases the curve intensity at large angle decreases. As the floc breakage is occurring the intensity tends to increase up to the un-aggregated bentonite one. This behaviour is modelized through the multiple scattering theory [26,27], by using the approximation of the mean field Mie scattering by fractal aggregates [31]. This approximation is validated by a comparison of the scattering and extinction cross sections values calculated using, on the one hand, Mie theory with a mean optical index ($\bar{n}$) and, on the other hand, the mean field approximation. By introducing the scatterers' mean optical index ($n_s/\bar{n}$) which varies during aggregation and floc breakage it is possible to modelize the form factor $F(q)$.

In this case Fig. 12 shows a 'reversibility' of the aggregation and the floc breakage corresponds to a continuous decreasing of the number of subunits (pristine bentonite particle) around each subunit without destabilizing the primary bentonite subunits.

3.3.3. Floc reformation

After breakage, the rotating speed was decreased to 60 rpm to determine floc re-growth capacity (Fig. 12). Floc re-growth kinetic is rapid and 3–5 min are sufficient to obtain a stabilized size. It appears that, for the operating conditions investigated, floc growth is never reversible. The percentages of reformation range 13–53% (Table 4). The re-growth percentage decreases when the shear stress that was applied to break the flocs increases. This may be due to polymer reconformation. For coagulant C577 and C595, concentration that gives the larger flocs is also the one that allows the best floc reformation. The polymer of highest molecular weight (C595) induces a slightly better reformation rate than C591, indi-

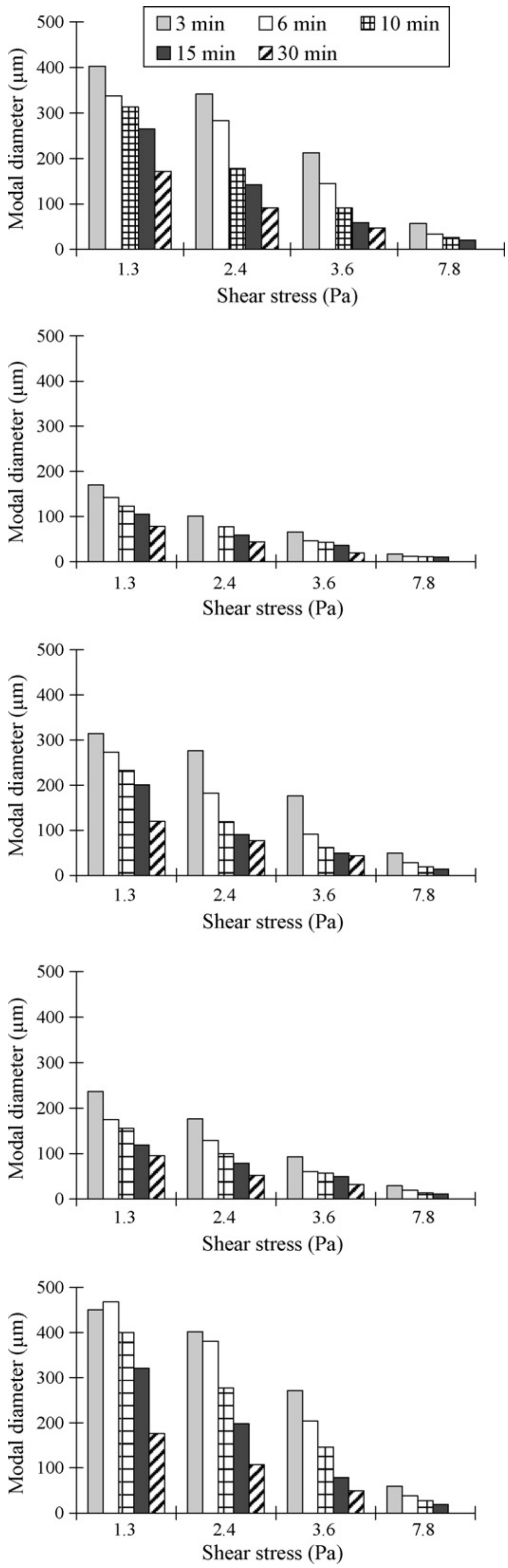

Fig. 11. Variations of floc modal diameter and fractal dimension versus shear stress in Taylor–Couette reactor B: (a) C591 at 0.19 ppm, (b) C577 at 0.19 ppm, (c) C577 at 0.49 ppm, (d) C595 at 0.15 ppm, and (e) C595 0.39 ppm.

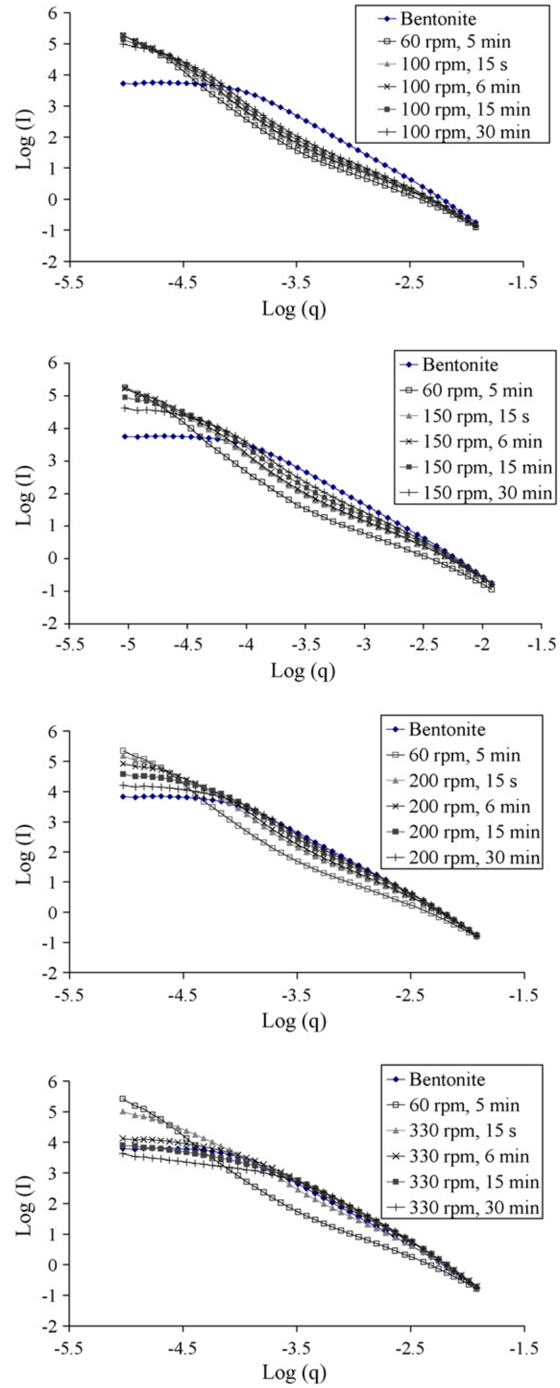

Fig. 12. Variations of log(I) versus log(q) during deaggregation in Taylor–Couette reactor B at different rotating speed [C595 at 0.39 ppm].

cating that polymer chain length could influence floc reformation capacity. However, authors have shown that even mineral coagulants inducing only charge neutralization do not enable a total reformation of flocs after their breakage, even when shear stress is maintained during a short period [4,9].

4. Conclusion

A protocol was developed to determine aggregate behaviour under a wide range of shear stresses. The study of coagulation during Jar-test and in Taylor–Couette reactors shows a clear difference between organic and mineral coagulants. Early age floc growth kinetic for ferric chloride is more rapid than for polyelectrolytes. However, flocs formed by the metal salt are more easily broken by shear. They cannot resist to a medium shear stress equal to 1.5 Pa. Moreover, their fractal dimension is smaller than fractal dimension of flocs formed with polyelectrolytes, which can explain their less resistance to shear. Polyamine and polyDADMAC coagulants react differently to shear stress. A coagulant whose molecular weight is more important leads to the formation of more resistant flocs, certainly due to the bridging phenomenon that appears during coagulation. However, when the shear stress is increased to high value of 7.8 Pa, floc breakage is almost instantaneous for each coagulant, at each concentration. Floc re-growth after breakage ranges the same performance for each coagulant, but is dependant on coagulant concentration. However, reformation is never complete, and reformation percentage decreases when the applied shear stress increases. Fractal dimension measurements for coagulation induced by polyelectrolytes indicate that floc breakage mechanism in Taylor–Couette reactor is mainly particle erosion. Polyelectrolytes as polyamine and polyDADMAC have shown a strong ability to shear resistance compared to ferric chloride, for an equivalent efficiency to remove particulate matter. This type of coagulant would be more convenient for processes where high shear stress can occur. The study of a model bentonite suspension provides a good base for a better understanding of coagulation process. Bentonite flocs are subjected to different mechanical and hydrodynamic constraints, which lead to a change in their characteristics.

References

[1] L.A. Glasgow, R. Lucke, Mechanisms of deaggregation for clay–polymer flocs in turbulent systems, Ind. Eng. Chem. Fundam. 19 (1980) 148–156.
[2] P.T. Spicer, S.E. Pratsinis, The effect of impeller type on floc size and structure during shear-induced flocculation, J. Colloid Interface Sci. 184 (1) (1996) 112–122.
[3] P.T. Spicer, S.E. Pratsinis, Shear-induced flocculation: the evolution of floc structure and the shape of the size distribution at steady state, Water Res. 30 (5) (1996) 1049–1056.
[4] P. Spicer, S. Pratsinis, J. Raper, R. Amal, G. Bushell, G. Meesters, Effect of shear schedule on particle size, density, and structure during flocculation in stirred tanks, Powder Technol. 97 (1) (1998) 26–34.
[5] C. Selomulya, R. Amal, G. Bushell, T.D. Waite, Evidence of shear rate dependence on restructuring and breakup of latex aggregates, J. Colloid Interface Sci. 236 (1) (2001) 67–77.
[6] R.K. Chakraborti, K.H. Gardner, J.F. Atkinson, J.E. Van Benschoten, Changes in fractal dimension during aggregation, Water Res. 37 (4) (2003) 873–883.
[7] S. Yoon, Y. Deng, Flocculation and reflocculation of clay suspension by different polymer systems under turbulent conditions, J. Colloid Interface Sci. 278 (1) (2004) 139–145.
[8] D. Bouyer, C. Coufort, A. Liné, Z. Do-Quang, Experimental analysis of floc size distributions in a 1-L jar under different hydrodynamics and physicochemical conditions, J. Colloid Interface Sci. 292 (2) (2005) 413–428.
[9] P. Jarvis, B. Jefferson, S. Parsons, Floc structural characteristics using conventional coagulation for a high doc, low alkalinity surface water source, Water Res. 40 (14) (2006) 2727–2737.
[10] T. Li, Z. Zhu, D. Wang, C. Yao, H. Tang, Characterization of floc size, strength and structure under various coagulation mechanisms, Powder Technol. 168 (2) (2006) 104–110.
[11] V. Oles, Shear-induced aggregation and breakup of polystyrene latex particles, J. Colloids Interface Sci. 154 (2) (1992) 351–358.
[12] C. Selomulya, G. Bushell, R. Amal, T.D. Waite, Aggregate properties in relation to aggregation conditions under various applied shear environments, Int. J. Miner. Process. 73 (2–4) (2004) 295–307.
[13] C. Coufort, D. Bouyer, A. Liné, Flocculation related to local hydrodynamics in a Taylor–Couette reactor and in a jar, Chem. Eng. Sci. 60 (8–9) (2005) 2179–2192.
[14] B. Bolto, J. Gregory, Organic polyelectrolytes in water treatment, Water Res. 41 (11) (2007) 2301–2324.
[15] R. Sarika, N. Kalogerakis, D. Mantzavinos, Treatment of olive mill effluents. Part II. Complete removal of solids by direct flocculation with poly-electrolytes, Environ. Int. 31 (2) (2005) 297–304.
[16] B. Bolto, D. Dixon, R. Eldridge, S. King, Cationic polymer and clay or metal oxide combinations for natural organic matter removal, Water Res. 35 (11) (2001) 2669–2676.
[17] E. Chang, P. Chiang, W. Tang, S. Chao, H. Hsing, Effects of polyelectrolytes on reduction of model compounds via coagulation, Chemosphere 58 (8) (2005) 1141–1150.
[18] B. Lartiges, J.Y. Bottero, L.S. Derrendinger, B. Humbert, P. Tekely, H. Suty, Flocculation of silica with Al salts: an ^{27}Al solid state NMR investigation, Langmuir 13 (1997) 147–152.
[19] F. Mabire, R. Audebert, C. Quivoron, Flocculation properties of some water-soluble cationic copolymers toward silica suspensions: a semiquantitative interpretation of the role of molecular weight and cationicity through a "patchwork" model, J. Colloid Interface Sci. 97 (1) (1984) 120–136.
[20] Y. Zhou, G.V. Franks, Flocculation mechanism induced by cationic polymers investigated by light scattering, Langmuir 22 (16) (2006) 6775–6786.
[21] P. Bacchin, P. Aimar, V. Sanchez, Influence of surface interaction on transfer during colloid ultrafiltration, J. Membr. Sci. 115 (1) (1996) 49–63.
[22] O. Morineau-Thomas, P. Legentilhomme, P. Jaouen, Improvement of the performance of the ultrafiltration of bentonite suspensions using a swirling decaying annular flow: comparison with tangential plane and axial annular flows, J. Membr. Sci. 193 (1) (2001) 19–33.
[23] R. Moll, D. Veyret, F. Charbit, P. Moulin, Dean vortices applied to membrane process. Part I. Experimental approach, J. Membr. Sci. 288 (1–2) (2007) 307–320.
[24] P. Luckham, S. Rossi, The colloidal and rheological properties of bentonite suspensions, Adv. Colloid Interface Sci. 82 (1–3) (1999) 43–92.
[25] E. Barbot, S. Moustier, J.Y. Bottero, P. Moulin, Coagulation and ultrafiltration: understanding of the key parameters of the hybrid process, J. Membr. Sci. 325 (2008) 520–527.
[26] G.I. Taylor, Stability of a viscous liquid contained between two rotating cylinders, Trans. R. Soc. (1923) 223–289.
[27] S. Lambert, A. Thill, P. Ginestet, J.M. Audic, J.Y. Bottero, Structural interpretations of static light scattering patterns of fractal aggregates. I. Introduction of a mean optical index: numerical simulations, J. Colloid Interface Sci. 228 (2) (2000) 379–385.
[28] R.J. François, Strength of aluminium hydroxide flocs, Water Res. 21 (1987) 1023–1030.
[29] P. Jarvis, B. Jefferson, J. Gregory, S.A. Parsons, A review of floc strength and breakage, Water Res. 39 (2005) 3121–3137.
[30] A. Thill, S. Moustier, J. Aziz, M.R. Wiesner, J.Y. Bottero, Flocs restructuring during aggregation: experimental evidence and numerical simulation, J. Colloid Interface Sci. 243 (1) (2001) 171–182.
[31] R. Botet, P. Rannou, M. Cabane, Mean-field approximation of Mie scattering by a fractal aggregates, Appl. Opt. 36 (1997) 8791–8797.